Experimental analysis and quantification of air infiltration into a passenger car cabin

Matisse Lesage, David Chalet, Jérôme Migaud

Experimental analysis and quantification of air infiltration into a passenger car cabin

Matisse LESAGE[1] *, David CHALET[1], Jérôme MIGAUD[2]

[1]Ecole Centrale de Nantes, LHEEA lab. (ECN/CNRS), Nantes, France
[2]MANN+HUMMEL France, Laval, France

(*) corresponding author
Address: 1 rue de la Noë 44321 Nantes, France
Mail: matisse.lesage@ec-nantes.fr
Phone: +33 (0)2 55 58 90 11

Abstract

Nowadays, air quality in closed environments is of major interest, particularly in very small volumes such as car cabins. In typical driving conditions, ambient air enters by infiltration as the vehicle speed increases. In order to satisfy more ambitious requirements on air quality and energy savings, it is necessary to evaluate the infiltration risk. At first, an experimental method is created to identify the infiltration path in the cabin of a moving car. On a modern electric vehicle, the privileged path is observed at the front of the cabin near the feet of the front passengers. A second experimental campaign is performed to quantify the infiltration flow rate. Results show that the flow rate is not negligible as it can reach several dozen kilograms per hour. The ventilation settings (blower speed and recirculation ratio) can be managed to reduce or even completely remove infiltration in some cases.

Keywords

Infiltration, Leakage, Ventilation, Air quality, Tracer gas

Nomenclature

Q	Volumetric flow rate (m^3/h)
t	Time (s)
V	Cabin volume (m^3)
C(t)	Mass fraction concentration

Subscripts

amb	Ambient (outside environment)
CO_2	Carbon dioxide

Acronyms

GPS	Global Positioning System
GRG	Generalised Reduced Gradient
HVAC	Heating, ventilation and air-conditioning
NEDC	New European Driving Cycle
WLTC	Worldwide Harmonised Light Vehicle Test Cycle

1. Introduction

Heating, ventilation and air-conditioning (HVAC) system plays a major role in the thermal comfort (Lesage et al., 2019b) and air quality of car cabins (Mathai et al., 2020; Migaud et al., 2018). It also has a safety aspect regarding the windshield defogging. In modern vehicles, the HVAC system is managed either manually by the passengers or automatically by the on-board control system. Depending on the outside conditions (temperature, humidity, pollution) the amount of air driven by the blower can be adjusted, as well as the portion of recirculated air compared to fresh air. In addition to this controlled airflow, there can be another uncontrolled airflow from the outside into the cabin: infiltration. The terminology related to airflows considered in the article is shown in Figure 1.

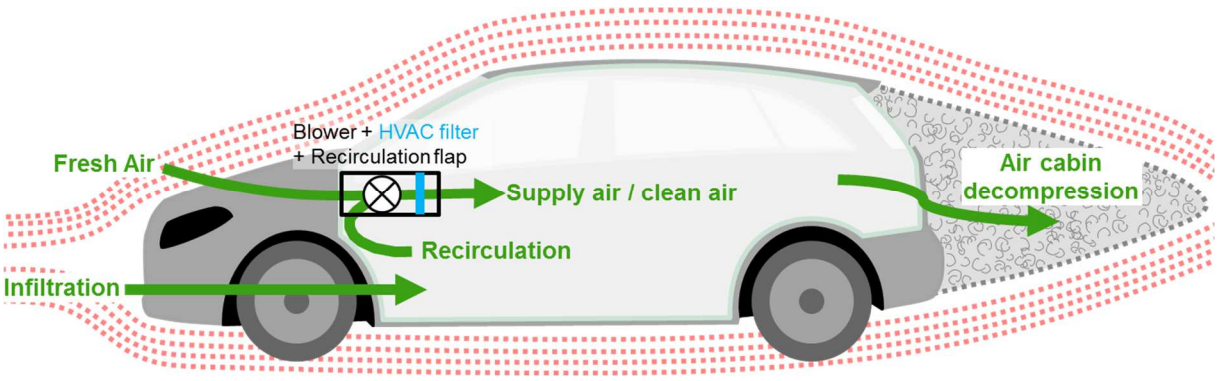

Figure 1 Overview of the air circulation in and out of a passenger car

The "infiltration" term refers to the air entering the cabin by other means than the blower operation. This word has a similar meaning than the words "intrusion" or "penetration". Depending of its intensity, infiltration can have a wide impact on the cabin system. Indeed one can build a perfect filtration system in the ventilation circuit, it remains pointless if the air enters the cabin by other means. This issue is also important concerning the energy aspect. The thermal balance can be influenced as more outside air enters the cabin. The infiltration phenomenon must not be neglected as it can introduce a significant amount of air, particularly at high vehicle speeds. The objectives of this study is to understand the infiltration process and quantify the flow rate driven. Eventually the work presented in this paper can help to offer solutions: either change the vehicle manufacturing process to achieve an airtight car body, or apply a strategy to the ventilation system to limit the infiltration flow rate. The benefits could be important either on the air quality or on the energy consumption.

At first, this article presents the state of the art found in the literature regarding infiltration. Then experiments are realised on a modern electric vehicle in order to identify the air paths as it exits or enters the cabin. The localisation of infiltration on this vehicle leads to reconsider the models found in the literature. An experimental campaign is realised on two modern vehicles to evaluate the infiltration flow rate in driving conditions.

2. Literature review

The literature research shows that infiltration is not a widespread phenomenon in the automotive field. Most findings concerning the infiltration of air in a closed volume is for building applications. Old or recent studies investigate the characterisation of airflow through cracks, with a pressure approach (Baker et al., 1987; Lv et al., 2018). Equations are created to

link the pressure drop and the flow rate. The most common use a power law, but the authors advocate for a quadratic equation as a better and more general equation to describe crack flow. These equations are verified with experiments for different crack geometries and a large range of Reynolds number. The characterisation of infiltration in buildings can also be evaluated with means of gas tracer methodology (Heidt and Werner, 1986). The monitoring of a gas concentration is used to calculate the air exchange rate within a room. Both the pressure approach and the gas tracer methodology could be applied to vehicles.

One of the few studies with a vehicle application is the work of Xu et al. (2010). It investigates the penetration of particles through different crack geometries in the car body. The authors point out the high influence of this infiltration over the cabin air quality. However, the investigation is not made with a moving car but in static conditions. Another study explores the influence of the vehicle velocity on the ventilation system (Fišer and Pokorný, 2014). The authors built a thermal model to predict the cabin heat load. They point out that the vehicle velocity has high influence on the model accuracy, particularly at high speed. A possible cause could be a dependency between the amount of air exchange rate and vehicle speed. The authors do not investigate the infiltration issue.

Several studies suggest that the cabin pollution level is correlated to exhaust intrusion elsewhere than through the blower (Chan et al., 1999; Fruin et al., 2011; Harik et al., 2017; Hudda and Fruin, 2013). There is a debate whether this penetration occurs at the front of the cabin through the firewall (Abi-Esber and El-Fadel, 2013; Chan and Chung, 2003) or near the trunk (Behrentz et al., 2004; Zagury, 2000). This is important to know if the infiltration air is polluted by the vehicle itself (self-pollution through the trunk) or by the upfront vehicle (infiltration at the front). It should be noted that these studies focus on the pollution level within the cabin rather than the infiltration effect itself or any attempt to quantify it.

A detailed methodology to measure infiltration flow rate is found in the work by Knibbs et al. (2007). This is an experimental investigation of the air flow rates with different ventilation settings and vehicle velocity. The authors used a tracer gas methodology with sulphur hexafluoride (SF_6). The study is made with cars of different types: small hatchback, sedan, pick-up truck and large hatchback. Two cars are from 1989 and 1998 with high mileage (> 120 000 km) while two cars are both from 2005 and in relatively new condition (< 8 000 km). Tests are performed at 0, 60 and 110 km/h with four ventilation settings. The test results

indicate that the flow rate increases with vehicle speed, particularly for older vehicles. From lowest to highest vehicle speed, the air flow rate can be increased by up to 150 m^3/h for the 1989's car, and around 30 m^3/h for the 2005's cars. The experiment is repeated with two additional vehicles (Knibbs et al., 2009). Authors explain that the blower operation is likely to reduce the infiltration flow rate. Infiltration appears in recirculation mode as well as in fresh air mode. This infiltration has a negative impact on the particle level within the cabin.

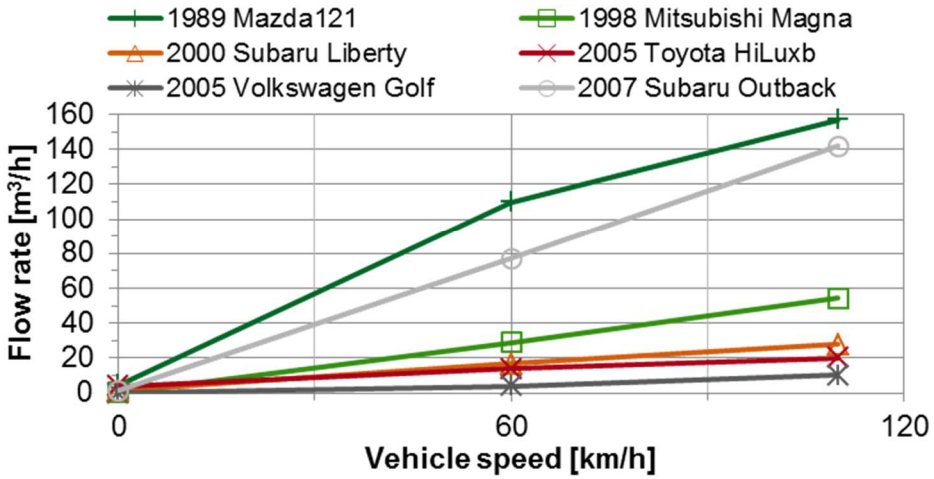

Figure 2 Evidence of infiltration in 6 vehicles from Knibbs et al. (2009, 2007)

Similar methodology has been used in several older studies using CO or SF_6 as the tracer gas in passenger cars (Conceição et al., 1997; Fletcher and Saunders, 1994; Ott et al., 1994; Petersen and Sabersky, 1975) and school buses (Behrentz et al., 2004; Ireson et al., 2004; Marshall and Behrentz, 2005). All studies confirm an increase of the air exchange rate with vehicle speed. Fletcher and Saunders (1994) find that the wind speed and direction have a low influence on infiltration compared to the influence of vehicle speed. Overall, the vehicle samples are limited, as well as the maximum speed and the ventilation settings. A couple of studies use CO_2 (Park et al., 1998), N_2O (Clifford et al., 1997) or alcohol (Engelmann et al., 1992; Ott et al., 2008) as a tracer gas but only in stationary conditions.

The most complete and detailed work on infiltration is performed by Lee et al (Lee, 2013; Lee et al., 2015a, 2015b; Quiros et al., 2013; Zhu and Lee, n.d.). The global approach relies on the pressure competition in and out of the cabin. According to the authors, the infiltration flow rate can be calculated knowing two differential pressures (cabin and aerodynamic).

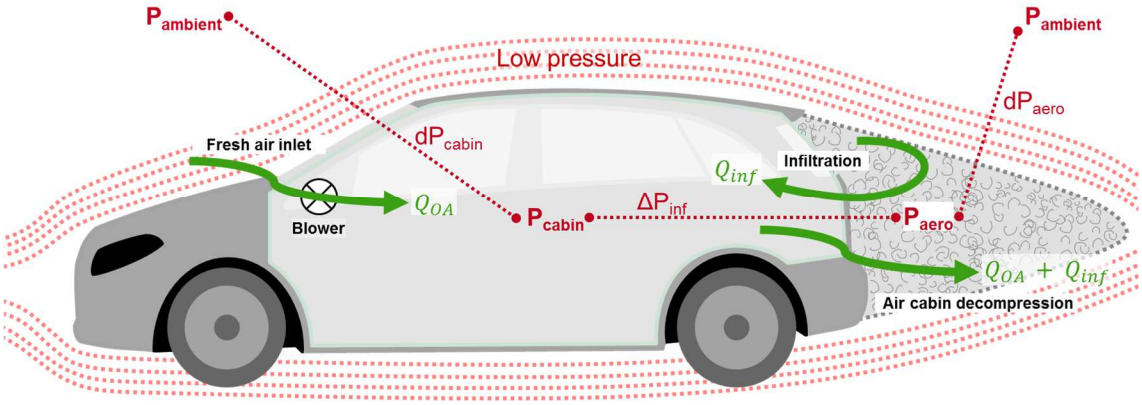

Figure 3 Cabin pressurisation and infiltration model adapted from Lee studies

Experimental tests with a broad range of vehicles (sedan, hatchback, SUV, minivan) led to repeatable outcomes. Tests are performed with a moving vehicle (up to 120 km/h). A model is created from the test results. On the one side, the aerodynamic pressure can be calculated knowing the vehicle speed. On the other side, the cabin pressurisation depends on the flow rate of fresh air entering the cabin (itself depending on blower speed and recirculation ratio). Several correlation coefficients are used to adjust the model for each tested vehicle. The idea is that infiltration is triggered by the competition between the aerodynamic and cabin pressures: infiltration happens when the aerodynamic pressure is higher than the cabin pressure. According to the article the infiltration is located at the rear back of the cabin for all the studied vehicles.

In order to assess what could be the potential impact of infiltration on the cabin air quality in real driving conditions a computed scenario is performed. This one is developed with the vehicle X parameters (see part 3). The vehicle is in fresh air mode (recirculation OFF), and Lee's infiltration model based on its average vehicle is used. The calculation is performed on a normalised road cycle. The WLTC is a mixed cycle, with urban, suburban and highway parts, that replaced the NEDC as the most common procedure in Europe. This cycle covers most driving conditions in terms of vehicle speed. The infiltration results are presented on Figure 4.

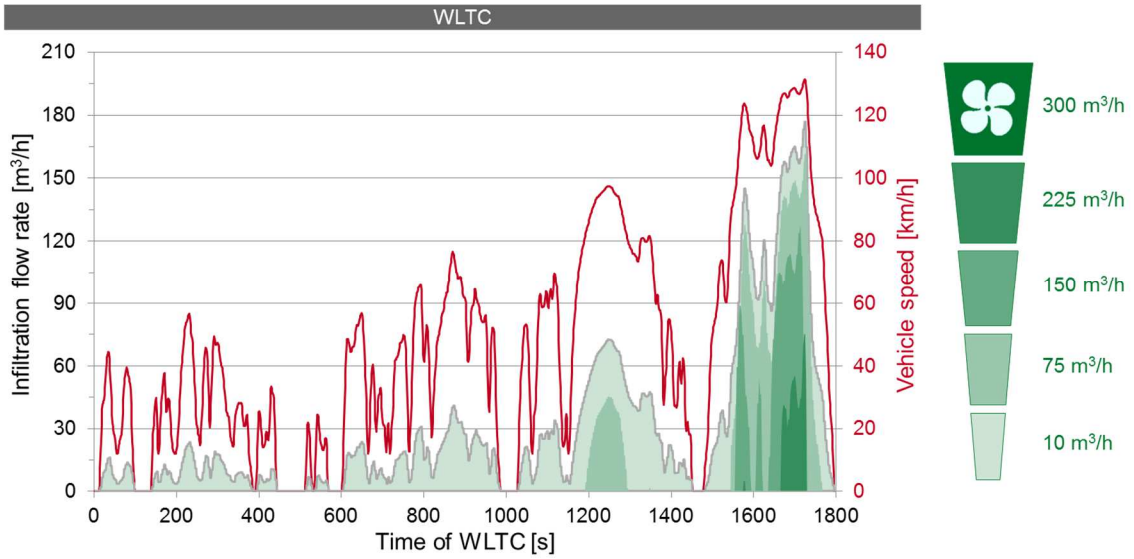

Figure 4 Results of infiltration flow rate with Lee's model on normalised driving cycle (WLTC) with various blower settings

On the road cycle, the infiltration occurs most of the time but at a reduced flow rate. With a blower setting at 10 m^3/h, the infiltration volume over the whole cycle (1800s) is 15 m^3. This is a very high amount compared to the air volume driven by the blower (5 m^3). As the blower flow rate increases, the infiltration decreases. At medium blower position (150 m^3/h) the infiltration does not appear before the final part of the cycle (highway). This setting is good for urban and suburban trips. With the blower at its maximum speed (300 m^3/h) there is no infiltration in the highway part either.

It appears that the infiltration can have a very high impact on the air circulating in the vehicle. In recirculation mode or at a low blower setting the infiltration air prevails in the cabin. A solution to reduce or even delete the infiltration is to increase the amount of fresh air driven by the blower. According to Lee's model, this allows creating an overpressure in the cabin that acts as a shield against infiltration. Lee's studies do not include experiments on modern or electric vehicles. Hence, this model must be checked and/or adapted. In that purpose several experiments are performed, described in the following sections.

3. Experimental identification of leakage and infiltration paths

The experiments are performed with a full electric vehicle from 2018 with a total mileage of 3800 km. It is referred to as "vehicle X". All tests are performed at ordinary ambient temperature (19-25°C) and relative humidity (40-60%).

At first, the idea is to acquire knowledge on the exchange of air between the cabin and its surrounding environment. In that regard, it is important to identify the leakage path(s), from the cabin to the outside, and the infiltration path(s), from the outside to the cabin. The outside air driven by the blower into the cabin is not included in the "infiltration" term, but rather as a "fresh-air inlet" (as depicted on Figure 1). Indeed the fresh-air inlet flows through the HVAC system comprising the filters and heat exchangers, while the infiltration is an unwanted and uncontrolled airflow allegedly introducing pollutants, particles and disturbing the thermal balance of the cabin.

Tests are performed in static condition (0 km/h). The vehicle is placed in a room which ventilation system can be deactivated by the operator. Hence, the tests are not influenced by any uncontrolled external airflow (e.g. wind). For information, the vehicle cabin volume is 2.5 m^3 (specification from manufacturer), and the raw volume of the room (i.e. empty) is approximately 90 m^3. As depicted in Figure 5, the vehicle is mounted with a fake window adaptation in order to inject air into the cabin (leakage tests) or to suck air (infiltration tests). The shape and dimensions of the fake window is the same as the top part of the original window. The material selected is transparent polycarbonate, so that the hole can be drilled easily while maintaining good visibility. The fake window is placed on top of the original window, with airtight sealing tape at the junction. It is assumed that the sealing properties of the window are not altered. The blower ventilation path is blocked: ventilation grids are sealed with tape (as shown in Figure 5) and the HVAC system is placed in recirculation mode. This ensures no backward airflow in the blower circuit (this path is known). Otherwise, the vehicle is in its original configuration with all doors and windows closed.

Figure 5 Test setup to identify leakage and infiltration paths of vehicle X.

3.1 Leakage paths

For the leakage tests, a fog machine is used to generate smoke in the vehicle. Once the cabin is filled with smoke, clean air is injected through the fake window. Different methods and tools are used to identify the leakage paths (i.e. smoke) at the outside of the vehicle. The leakage points are found mostly by observation, with the help of a flashlight and a laser to better identify the minor leakage points. Besides, the smoke creates a huge increase of the particle concentration. Then a fine particle sensor (a TSI 8525 P-Trak) is navigated all around the car body to corroborate the observation method. This device counts the particles with diameter from 20 nm to 1 µm. The concentration in the ambient air is in the range of 5 000-10 000 particles per cubic centimetre, while it is up to 30 000-50 000 near smoke streams. Two types of leakage paths are identified:

- Main leakages, easily identifiable even at low flow rate of injected air
- 2nd order leakages that only occur for high inlet air flow rate (high cabin pressurisation)

The main leakages are located at the bottom of the rear trunk door, under the battery box below the vehicle, and above the rear wheels. They are explained by two factors. On the one side, the car body assembly is made mainly by rivet, which does not guarantee airtightness. On the other side, there is the decompression traps located above the rear wheels. On the studied car, these decompression traps are passive flaps that connect the outside environment

to the cabin. From the cabin inside one must remove the different garnish carpets in order to show the many holes in the car body that are connected to the decompression traps. Images extracted from different documentary video about manufacturing of modern electric vehicle illustrate the many holes in the car body that create a channel between the outside environment and the cabin (Figure 6). The vehicle is not designed to be airtight.

Figure 6 Decompression traps on various modern vehicles, and holes in the car body revealed during the manufacturing process (PlaneteGT TV, 2019; Motor.TV, 2017; manufacturing, 2013)

The 2nd order leakages only happen for very high cabin pressure and are not easily identifiable due to the low amount of smoke coming through these paths: near the side mirrors, at the top of the four side doors on the corner, and at the bottom of the front windshield through the HVAC inlet grid. The latter is probably a backward airflow coming through the ventilation circuit although caution is taken to prevent such event. It is possible that the high cabin pressurisation deforms the plastic parts of the HVAC box, which can create openings upstream the ventilation grids. The other 2nd order leakages are probably due to a deformation of the rubber door seal with the high cabin pressure. The flow rate of injected air is 40% higher than the maximum capability of the vehicle blower. Then the 2nd order leakages are unlikely to occur on real driving conditions. However, these areas should be checked over the

lifetime of the vehicle, as wear or deformation could enlarge these leakage paths. A summary of the leakage paths on the studied car is presented on Figure 7.

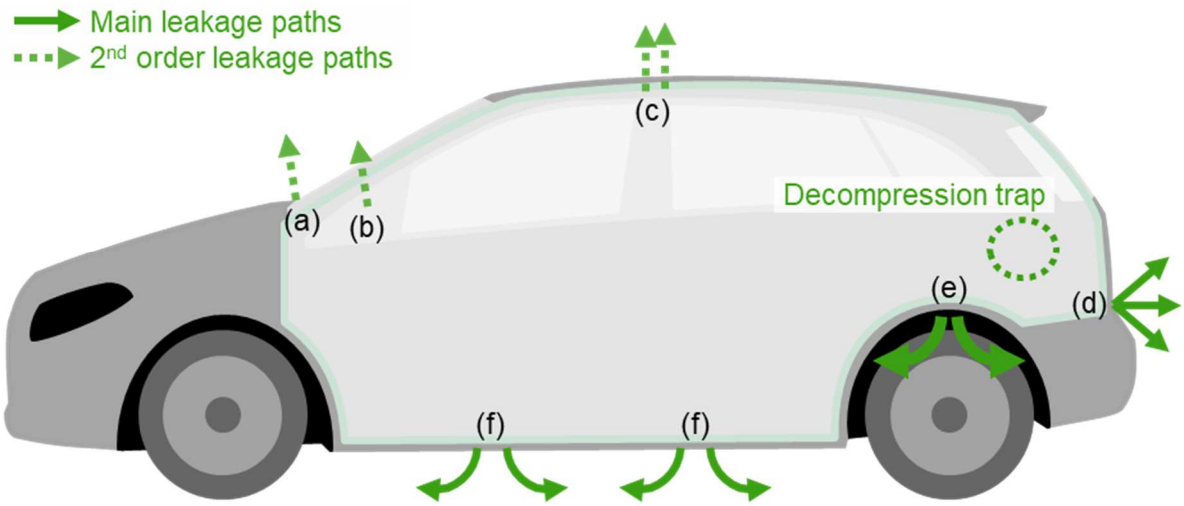

Figure 7 Leakage paths localisation: (a) bottom of the front windshield, (b) side mirrors, (c) top corner of the four side doors, (d) bottom of rear trunk door, (e) above rear wheels, (f) under battery box

3.2 Infiltration paths

The same setup as the leakage tests is used to identify the infiltration paths. Instead of injecting air through the fake window, an industrial vacuum cleaner is used to suck the cabin air at high flow rates. Different methods are used to identify the infiltration paths. At first, the operator is placed at the outside of the vehicle. The operator walks the active smoke generator all around the car while the cabin air is aspirated through the fake window. The objective is to observe (by visual inspection) a smoke stream infiltrating the cabin. Although it is clear that smoke enters the cabin by looking inside it through the windows, no clear stream is observed at the outside of the vehicle. Several methods are tested without success: variation of the operator-vehicle distance, variation of the smoke generation rate, and room lighting. Particular attention is given to the alleged infiltration paths (near the trunk, rear wheels, bottom of the vehicle, bottom of the front windshield) but no clear path is visible. A possible explanation is that the infiltration does not occur in one location at a high flow rate but at multiple locations at low flow rate.

In a second step, the operator is placed within the cabin. The room is filled with smoke and then the air is sucked in the vehicle. This methodology is more satisfactory than with the

outside operator, as the infiltration paths within the cabin are clearly noticeable. At the back of the vehicle, infiltration happens widely in the trunk through holes in the car body. Additional paths are witnessed at the bottom of rear seats on the door side, and through the seatbelt connection. These paths at the back of the vehicle are all connected to the decompression traps.

At the front of the vehicle, the infiltration paths are clearly visible below the dashboard, near driver and passenger feet. This infiltration stream is more important than at the back of the vehicle. Removing the carpet elements reveals several holes that could be connected to the outside, either below the car or at the front of it.

These tests are performed in static condition (0 km/h). In order to simulate the wind resistance, a big fan is placed in front of the vehicle. This 45 kW fan is normally used in a vehicle test bench facility. It does not act as a full aerodynamic facility (such as a wind tunnel). Still, it can create airflow with a velocity up to 130 km/h over a large diameter (1m). With the fan active, no infiltration is spotted in the trunk or near the rear seats. The only infiltration path detected, either with light, laser or particle sensor, is the one at the front of the cabin below the dashboard. An additional confirmation is obtained with a thermal camera. The temperature in the cabin is increased to a value higher than 40°C. The room temperature is kept at normal condition (23°C). The operator in the cabin examines the apparition of cold clusters. As depicted on Figure 8 the cold areas on the driver side quickly appeared behind the brake pedal and to the right of the accelerator pedal. These areas match the infiltration path observed with the smoke procedure. In the trunk or near the back seats no cold cluster is observed which leads to consider that in driving conditions there is no infiltration at the rear of the vehicle.

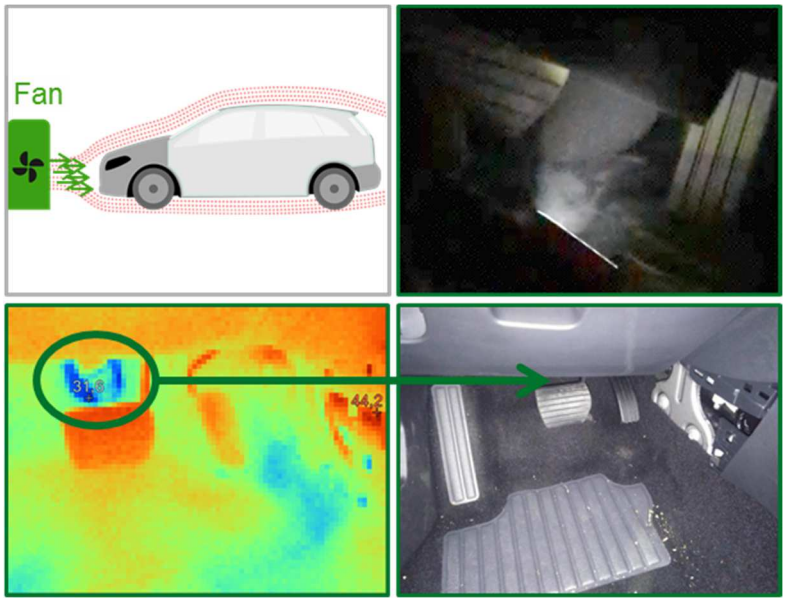

Figure 8 Identification of infiltration path at the front cabin bottom in replicated driving condition

This finding is not in accordance with several articles of the literature review (Behrentz et al., 2004; Zagury, 2000), including the work from Lee et al (Lee, 2013; Lee et al., 2015a, 2015b) which concludes that infiltration only occurs at the rear back of the vehicle in driving conditions. However, in the literature no experiment is found about modern or electric vehicles in new condition. There can be several important architecture and design differences between a traditional thermal vehicle and a modern electric vehicle. Lee's work includes many types of vehicle built between 2001 and 2013, with mileage from 1 900 to 261 000 kilometres. These factors might explain the difference in the infiltration location, since the geometry and design of the vehicle are believed to be a major factor in the infiltration process. In that regard the test procedure with the pressure approach cannot be applied to vehicle X. It is decided to use the tracer gas approach.

4. Evaluation of infiltration flow rate in driving condition with a tracer gas

4.1 Experimental setup and methodology

The aim of this test campaign is the characterisation of the infiltration flow rate in a moving vehicle. The idea is to evaluate the cabin air exchange rate by monitoring the carbon dioxide (CO_2) concentration (mass fraction). The use of CO_2 as a tracer gas to monitor air exchange rates within the vehicle cabin has already been done but in stationary condition (Park et al.,

1998) and with the uncertainty of the passenger breathing (Fruin et al., 2011). According to the Figure 9, the test procedure is divided in three stages:

- 1st step: increase the CO_2 level in the cabin (at least up to 1000 ppm), occupants breathe in the cabin in recirculation mode
- 2nd step: set the desired vehicle speed and ventilation settings for the test
- 3rd step: monitor the decay of CO_2 in the cabin while occupant(s) breathe(s) out of the cabin with a snorkelling tube

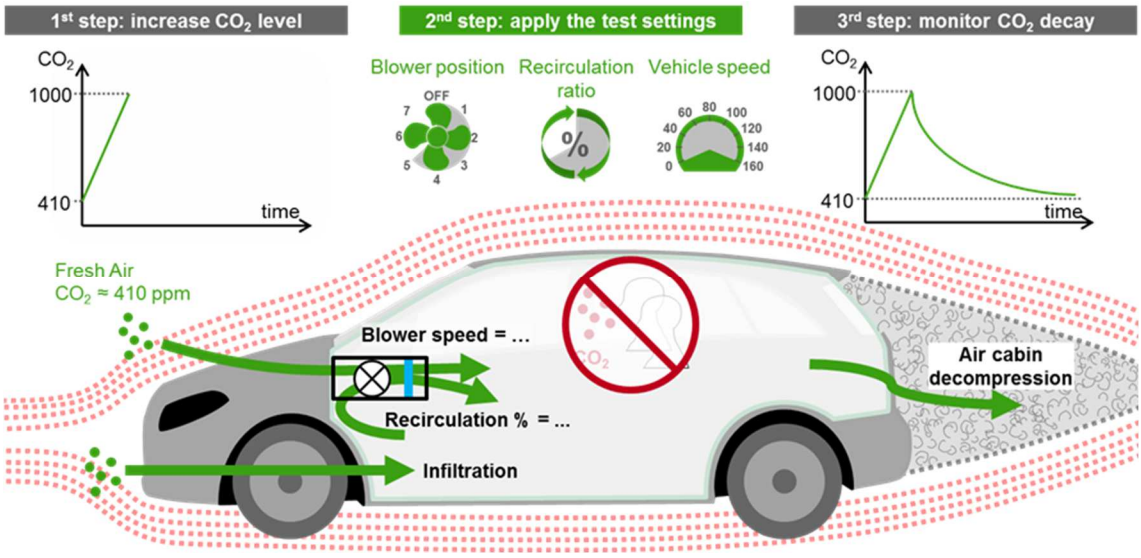

Figure 9 Methodology to evaluate infiltration using CO_2 as tracer gas

The methodology concept is based on the temporal decay of CO_2 concentration. Tracer gas techniques for single zone to measure the air exchange rate are described in the literature (Laussmann and Helm, 2011; Sherman, 1990). It can be described with the mass conservation equation. The differential equation is solved by integration.

$$V\frac{dC_{CO_2}(t)}{dt} = C_{CO_2\ amb} * Q - C_{CO_2}(t) * Q \quad \textbf{(1)}$$

$$C_{CO_2}(t) = C_{CO_2\ amb} + \left(C_{CO_2\ (t=0)} - C_{CO_2\ amb}\right).exp(\frac{Q.t}{-V}) \quad \textbf{(2)}$$

The cabin CO_2 concentration depends on the cabin volume V, the exterior CO_2 concentration $C_{CO_2\ amb}$ and the inlet volumetric flow rate from outside Q. These equations are applied with several assumptions:

a) Cabin is a perfectly homogeneous single-zone volume
b) Exterior (atmospheric) CO_2 concentration is constant in space and time
c) CO_2 is chemically stable and inert (no reactions with other molecules)

d) CO_2 is not absorbed by any cabin material (roof, seats, doors…)

e) No in-cabin source (nor sink) of CO_2 (driver does not inhale nor exhale within the cabin)

Assumption a) is the consequence of having a single CO_2 sensor but also to have data in order to develop a 0D model. This sensor is placed in the middle of the cabin between the four headrests. Within the cabin, the air is mixed by the air coming from the central ventilation grid, apart from for tests with blower off. The sensor is a Vaisala GMP343 with a response time (90%) of two seconds without the filter attached. Its accuracy in standard ambient conditions is +/- (5 ppm + 2% of reading).

For assumption b) no CO_2 sensor is placed outside the cabin to directly validate this statement. The exterior concentration is measured at the beginning of each test. Besides the final cabin CO_2 concentration converges toward the exterior concentration. The tests are time limited (a few minutes), thus space limited (a few kilometres). Because of these limitations, the final cabin stability is not reached for all tests. In cases that reached stability the initial and final CO_2 concentrations are similar with a +/- 7 ppm margin. It suggests that the atmospheric concentration is stable in time (over a few minutes) and space (a few kilometres).

Assumptions c), d) and e) induce that CO_2 concentration is only governed by air renewal. In other words, the cabin CO_2 level is only influenced by the flow rate of air coming from the outside to the cabin. This flow rate is the sum of the infiltration flow rate and the fresh air blower flow rate (itself depending on the blower position and recirculation ratio).

$$Q = Q_{blower\ fresh\ air} + Q_{infiltrations} \quad \textbf{(3)}$$

All equipment and test procedures are made to minimise the influence of test conditions on the infiltration phenomena. For instance, the installation of a flowmeter in the blower circuit would create a large pressure drop that could alter the blower performances. In that regard, the blower is characterised by a cabin differential pressure – flow rate calibration. It is a less intrusive method in two stages. On the one hand, a link is made between cabin pressurisation and flow rate injected by blowing air through the fake window. On the other hand, a link is made between cabin pressurisation and the vehicle ventilation settings by blowing with the blower at different positions. This methodology creates a link between the blower positions

and the flow rate of air injected. It allows knowing the fresh air blower flow rate for any ventilation settings. The experiment is repeated with two vehicles of the same cabin size range:

- Vehicle X (previously presented) from 2018, total mileage 3800 km
- Vehicle Y (gasoline engine) from 2016, total mileage 6000 km

Both models are relatively common in the automotive market amongst mid-size or compact vehicles (cabin of 2.5 m^3). Both cars are in their original configuration apart from the fake window installation. A hole is made in the fake window for the snorkelling system. During test recordings, the driver breathes in and out through a plastic tube. A nose clip is used to ensure that the breathing is made exclusively with the outside environment, thus not influencing the CO_2 level in the cabin. The CO_2 sensor and a temperature sensor are placed in the middle of the cabin, at equal distance of the four headrests. The acquisition unit and laptop are plugged on a battery. The GPS position is recorded to evaluate the vehicle speed with accuracy. It should be noted that both cars are equipped with cruise control, which allows keeping stable speed over time.

The tests are performed on open roads between the area of Nantes and Angers (France). The road selection and time of tests are selected to minimise wind influence and traffic conditions. However, random wind gust or passing cars can have an influence on the results. Static tests (0 km/h) are performed in a parking lot or within a ventilated room. Tests are performed at different vehicle speeds and ventilation settings (blower position and recirculation ratio):

- Blower speed: 3 positions (off, medium speed, full speed). On the dashboard, it corresponds respectively to positions 0, 4 and 8 for vehicle X, and positions 0, 3 and 6 for vehicle Y.
- Recirculation mode: 2 positions (ON/OFF). Distinct pressurization tests in static conditions (0 km/h) have confirmed that for both vehicles the ON position corresponds to a true 100% recirculation mode. It is not fully confirmed that the OFF position corresponds to a true 0% recirculation, although it is most likely the case.
- Vehicle speed: static (0 km/h) plus several speeds from 50 to 130 km/h

Each test lasts a few minutes (2 to 10 minutes). For all tests the initial cabin CO_2 concentration varies from 1200 to 1900 ppm. A total of 39 tests are performed with vehicle Y

(including 8 repeatability tests), and 24 tests with vehicle X (with no repeatability tests). The few tests performed twice are very consistent.

4.2 Test results and primary analysis

The results with the two vehicles lead to the same conclusions. Two main categories of CO_2 decay curves can be analysed. On the one hand, there are the recirculation OFF curves, with clear exponential decrease of concentration over time. In such cases the stability can be reached, with cabin concentration tending toward the exterior CO_2 level. On the other hand, there are the recirculation ON curves, with slow decrease of concentration. For these tests the stability is not reached in the given limited time slot (5 minutes). In all cases the concentration decreases over time. It suggests a flow of outside air coming into the cabin, either from the blower action or from infiltration. For the recirculation ON cases, the blower does not drive fresh air into the cabin, hence the CO_2 decrease is solely due to infiltration.

In order to illustrate the influence of vehicle speed on the results two examples are displayed in Figure 10. On the first chart, the ventilation settings are selected at medium blower position and recirculation mode. On the second chart, the blower is turned off, with recirculation flap in fresh air mode. These values are selected as an example. Similar analysis can be made with other ventilation settings.

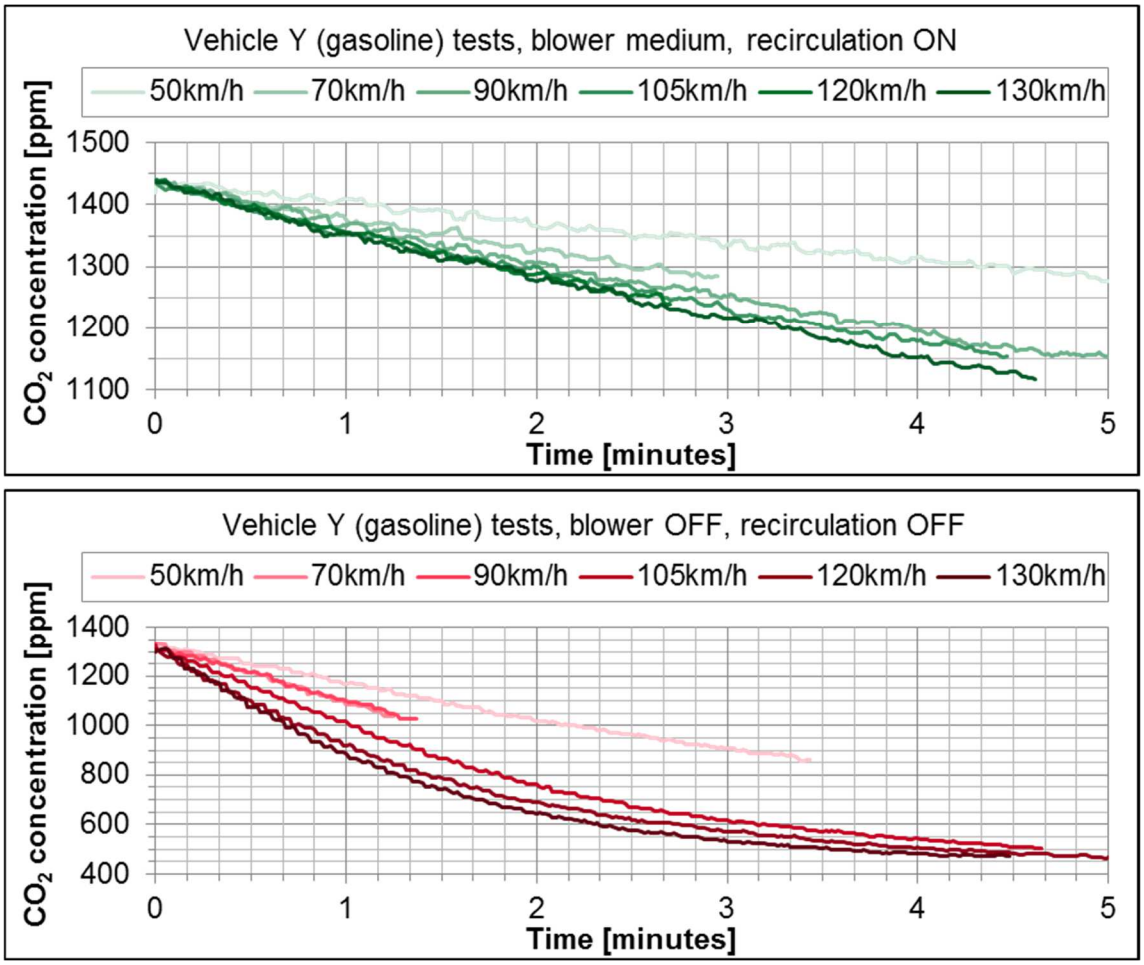

Figure 10 Influence of vehicle speed on cabin CO_2 decay

For both ventilation settings, the initial cabin concentration is the same for all tests (respectively 1440 and 1315 ppm). Six vehicle speeds are compared. A clear influence can be observed, with a quicker decrease of concentration as the speed increases. In recirculation mode at medium blower position, after 3 minutes the cabin CO_2 concentration decreases from 1440 ppm to 1330 ppm at 50 km/h, and down to 1215 ppm at 130 km/h. In fresh air mode with the blower turned off (bottom chart), after 3 minutes the CO_2 level drops from 1315 ppm to 910 ppm at 50 km/h, and down to 535 ppm at 130 km/h. At given ventilation setting the slope is higher when the vehicle speed increases. These results suggest that the infiltration flow rate increases with vehicle speed.

Similarly, the results can be displayed for a fixed vehicle speed and with varying ventilation settings. An example of the results at 105 km/h with vehicle Y is presented on Figure 11. The bottom curves represent the fresh air mode while the top curves are the recirculation mode. For each mode the blower position is set at 0 (blower off), 3 (medium position) and 6 (full

speed). In recirculation mode, the curve slopes are similar although not identical: the CO_2 decreases slightly more rapidly with upper blower positions. In fresh air mode, the influence of blower position is more obvious, and in agreement with what can be expected: the cabin CO_2 concentration decreases more rapidly when the blower drives more fresh air into the cabin.

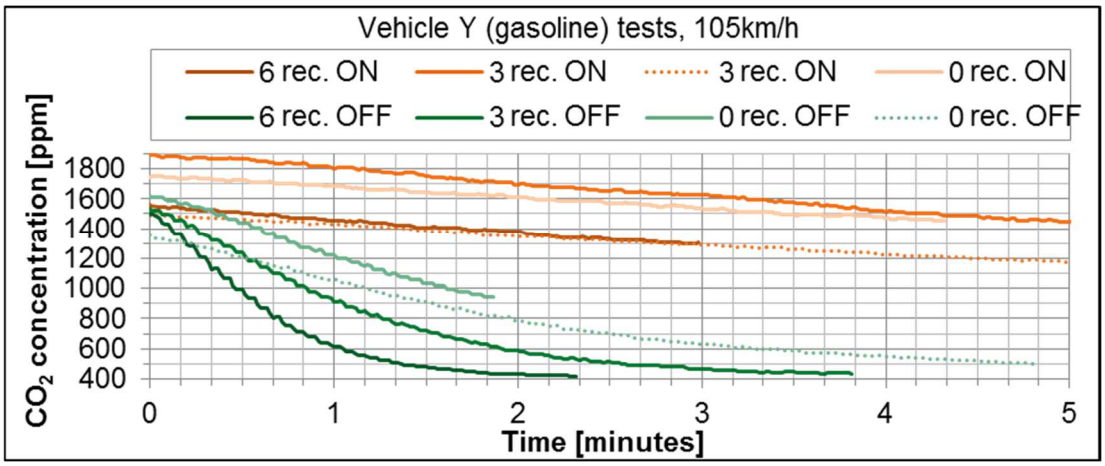

Figure 11 Influence of ventilation settings on cabin CO_2 decay

An interesting takeout from this chart is that there is a clear difference between the two curves with the blower off. If the recirculation flap is open (recirculation ON) the cabin CO_2 level decreases slowly, in the same range as when the blower is active. If the recirculation flap is closed (fresh air mode) the CO_2 decreases rapidly. It suggests that part of the infiltration path must be through the HVAC system of the vehicle. This phenomenon is observed for vehicle Y but not for vehicle X, as illustrated on Figure 12. For vehicle X the CO_2 curve slope with the blower turned off is almost identical whether the recirculation mode is activated or not. For this vehicle it suggests infiltration path must not be through the HVAC system, as opposed to vehicle Y. This is verified for all vehicle speeds (> 0 km/h) on both vehicles. Beside the fact that each vehicle has its own architectural design for the HVAC system, the difference could be explained by the control strategy applied to the recirculation flap.

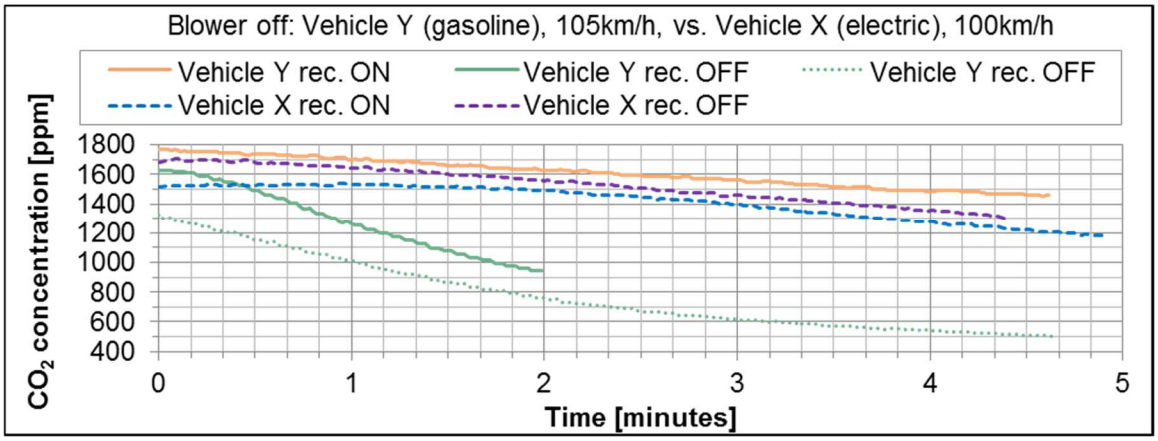

Figure 12 Comparison of vehicles X and Y with blower off

Several tests are performed in static condition (0 km/h), either in a room or on a parking lot area with minimum wind. The results show a temporal decay of CO_2. It induces that there is still an air renewal in the cabin although the lack of external flow rate removes the possibility for infiltration. This must be a consequence of diffusion effect, the vehicle is not airtight. Nevertheless, the CO_2 decay at 0 km/h is very slow compared to higher vehicle speeds. For vehicle Y with the blower off, the recirculation curve has the same slope as the fresh air mode curve, which is not the case when the vehicle is moving. It remains logical, because there is no infiltration, only diffusion. For both vehicles the diffusion is accelerated with higher blower flow rates. Indeed the airflow created by the blower allows achieving a better homogeneity within the cabin, particularly near the decompression flaps which can be considered as privileged places for diffusion.

4.3. Evaluation of infiltration flow rate

Experiments with the gas tracer methodology show that, for a given ventilation setting, the cabin air renewal rate depends on vehicle speed. This is due to infiltration phenomena. The next objective is to create an infiltration model that could be used in a simulation code. The first step is the evaluation of the infiltration flow rate in both vehicles (X and Y). The methodology used is the curve fitting of the test results with equation (2). The parameters to adjust the model are the ambient CO_2 concentration, the cabin volume and the outside air flow rate which is divided between the blower fresh air and the infiltration. The ambient CO_2 concentration is measured at the beginning of each test and allegedly constant over time. In fresh air mode, the blower flow rate is known for each position according to the cabin

differential pressure – flow rate calibration. It is assumed that this flow rate is independent of the vehicle speed. In recirculation mode, this flow rate is null. The two remaining unknown parameters to adjust the model are the cabin volume and the infiltration flow rate. The raw cabin volume of each vehicle is known, but is reduced because of the equipment and occupant(s). Then the cabin volume is used as a calibration parameter, within a reasonable range below the raw volume. A constraint is added that the same volume must be selected for all tests. Indeed, there is the same equipment and constant number of occupants for all tests in each vehicle (only the driver in vehicle X, two occupants in vehicle Y). Finally, the infiltration flow rate is adjusted for each test. This last step is pictured on Figure 13 with two examples of calibration for vehicle Y (recirculation ON or OFF). The idea is to minimise the difference with the test result. In that purpose, a solver (with GRG nonlinear method) is used to optimise the infiltration flow rate in order to minimise the error between the test result and the fitting equation. Other examples of curve fittings are presented on Figure 14 and Figure 15.

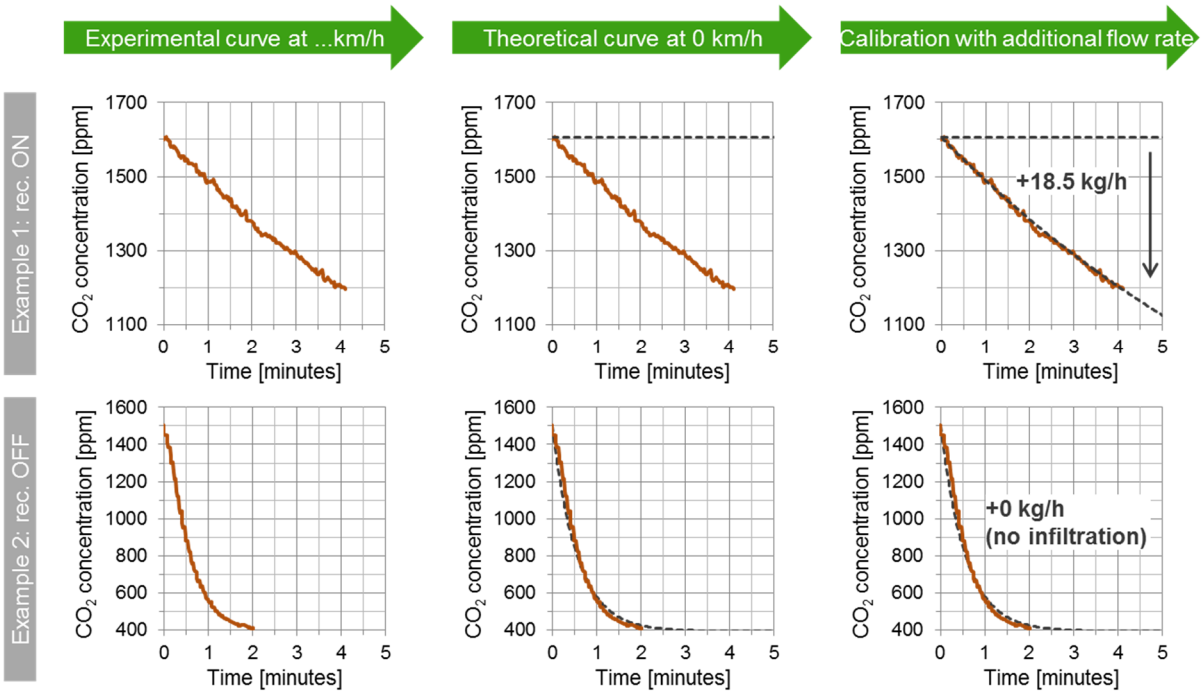

Figure 13 Simplified description of the process to estimate the infiltration flow rate

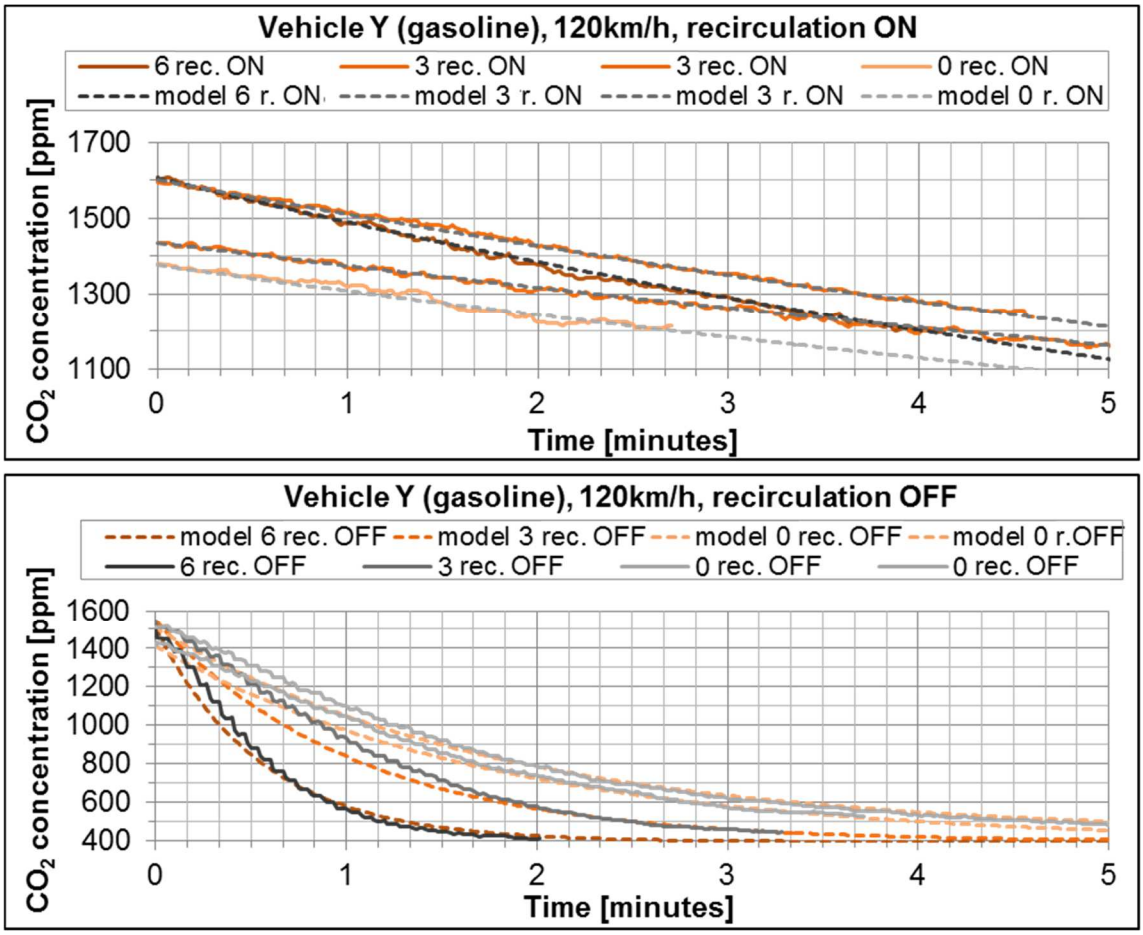

530

531 **Figure 14 Examples of curve fitting with vehicle Y tests at 120 km/h**

532

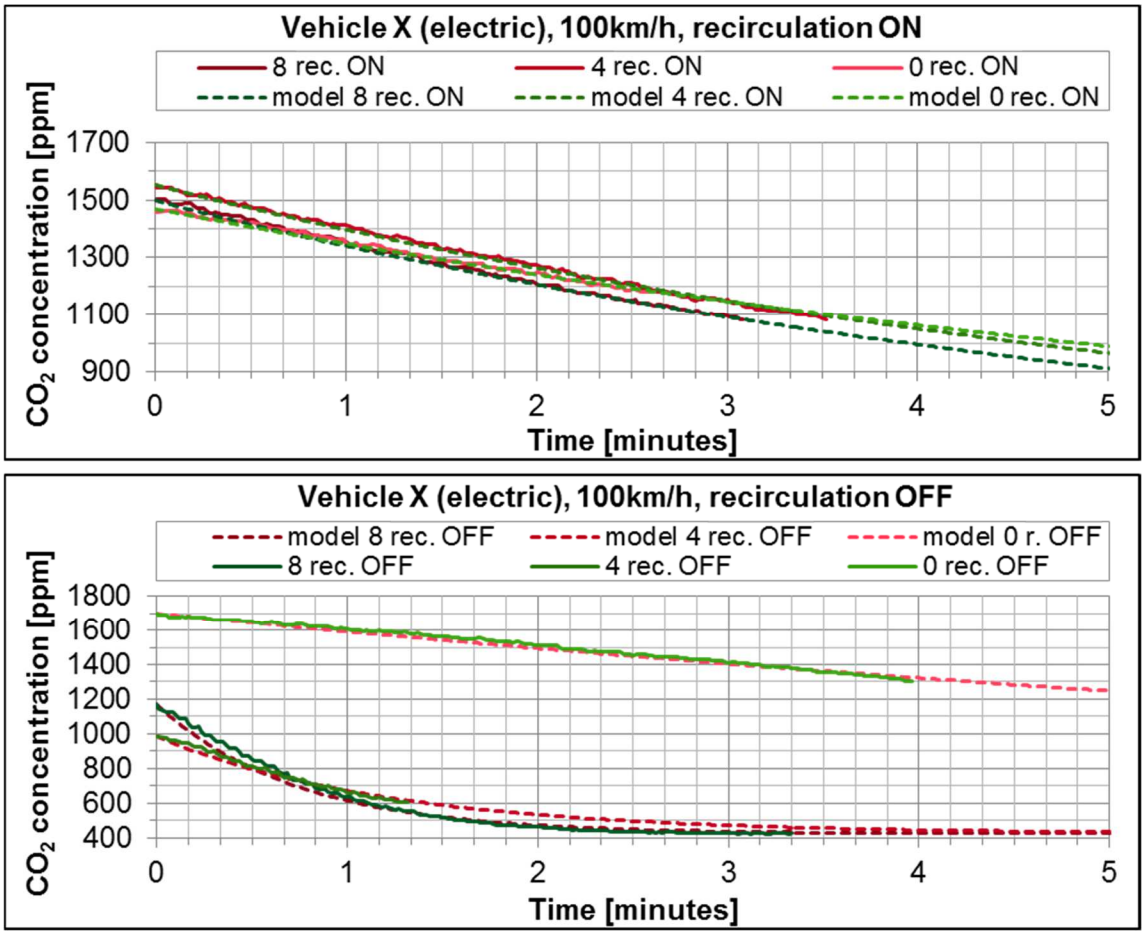

Figure 15 Examples of curve fitting with vehicle X tests at 100 km/h

The overall curve fitting of test results with equation (2) is very acceptable. For vehicle Y the average relative error is 1.7% (about 27 ppm) with a 2.1% standard deviation. This calculation takes into account the measurement uncertainty from the CO_2 sensor. 18 of the 39 tests have an average relative error below 1%, and 10 tests have an error above 3%. The 8 tests performed twice with vehicle Y lead to similar infiltration flow rates with a 5% relative error margin. The test methodology can be considered robust and repeatable. For vehicle X the average relative error is 1.6% (about 16 ppm) with a 1.8% standard deviation. 9 of the 24 tests have a relative error below 1% and 5 tests are above 3%. No repeatable tests are performed with vehicle X. Tests with this vehicle started with lower initial cabin CO_2 concentration in average (1349 ppm) than with vehicle Y (1502 ppm).

All the resulting infiltration flow rates of both vehicles are presented on Table 1 and Table 2. In recirculation mode, the infiltration is triggered by higher vehicle speeds and upper blower position. In fresh air mode, infiltration only happens with the blower off and increases with

higher vehicle speeds. In fresh air mode with an active blower the results are displayed with an asterisk "*" in the table. At first, it seems that there is no infiltration (0 kg/h) for these configurations, such as illustrated on the second example of Figure 13. However, there are several physical phenomena at stake (infiltration action, blower action, diffusion time in the cabin…) combined with some unpredictability about the exact position of the recirculation flap (not measured). Then an accurate identification of the infiltration flow rate appears uncertain for these configurations. Further experiments could help refine the experimental data set and thus improving the overall model accuracy. Yet the original vehicle configurations are limited in the range of recirculation ratio and blower flow rate that can be manually actuated on the dashboard. Such experiment would require a direct control on each actuator, for example with a connection to the vehicle control system.

Table 1 Estimation of infiltration mass flow rate on a gasoline vehicle for different ventilation settings and vehicle speeds

Infiltration mass flow rate vehicle Y [kg/h]							
Recirculation ON				Recirculation OFF			
GPS speed [km/h]	Blower position [0-6]			GPS speed [km/h]	Blower position [0-6]		
	0	3	6		0	3	6
0	3.5	4.0	6.0	0	2.5	-	-
46.7	-	6.0	-	46.7	35.0	-	-
66.5	-	9.5	-	66.5	48.0	-	-
87.0	11.0	13.5	15.0	87.0	60.0	-	*
101.4	10.0	12.8	16.0	101.4	68.7	*	*
116.3	13.0	12.8	18.5	116.3	100.5	*	*
126.1	17.0	16.0	19.0	126.1	117.5	*	*

Table 2 Estimation of infiltration mass flow rate on a modern electric vehicle for different ventilation settings and vehicle speeds

Infiltration mass flow rate vehicle X [kg/h]							
Recirculation ON				Recirculation OFF			
GPS speed [km/h]	Blower position [0-8]			GPS speed [km/h]	Blower position [0-8]		
	0	4	8		0	4	8
0	1.0	6.5	10.5	0	2.0	*	*
73.2	8.5	24.0	26.0	73.2	8.0	*	*
96.9	22.5	27.0	29.0	96.9	16.0	*	*
116.8	27.0	32.0	38.0	116.8	24.0	*	*

The main difference between the two vehicles is when the blower is not active. The infiltration flow rate of vehicle X is very similar in recirculation mode and fresh air mode. It means that the infiltration path is likely to be the same in both modes. This path must not be part of the HVAC circuit, thus the infiltration air is not filtered by the HVAC filter. Infiltration introduces polluted air into the cabin. Vehicle Y leads to much higher infiltration flow rates in fresh air mode than in recirculation mode (factor 7). As previously stated this suggests that the infiltration path in fresh air mode goes largely through the HVAC pipes, contrary to the electric vehicle X. Chances are that this air goes through the filters, acting as if the blower is active. Infiltration introduces filtered air into the cabin. The difference between the two vehicles for this specific ventilation setting is illustrated on Figure 16.

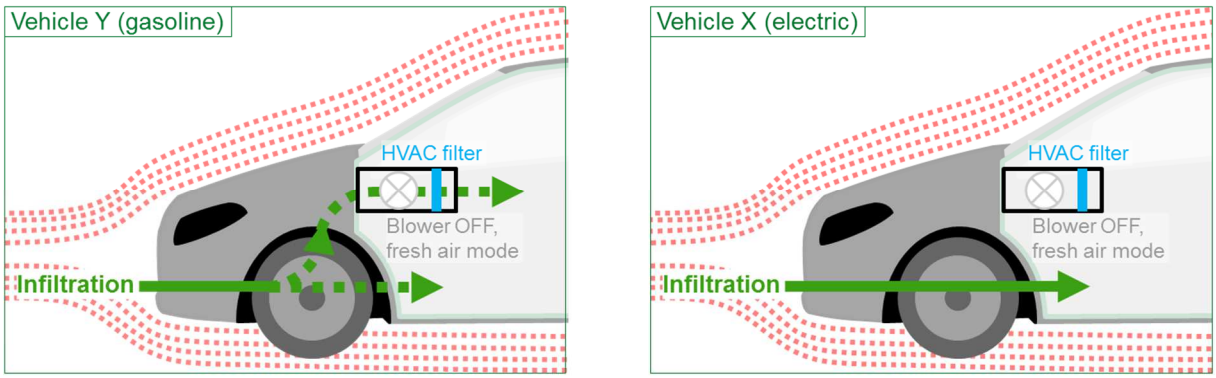

Figure 16 Infiltration path on vehicle X and Y in fresh air mode with blower OFF configuration

In recirculation mode, it appears that there is a higher infiltration flow rate with vehicle X than with vehicle Y, particularly at high vehicle speed. For both vehicles and at a given vehicle speed the infiltration flow rate slightly increases with upper blower position. The explanation might be that the air is better mixed within the cabin with higher blower position. Similarly than for the diffusion effect at zero vehicle speed this could stimulate the air renewal near interior-exterior border locations such as the decompression traps.

Otherwise, in recirculation mode the vehicle speed has a high influence on the infiltration flow rate. A trip on a highway (110 to 130 km/h) generates up to a dozen more kilograms per hour infiltration flow rate than a trip on a local road (60 to 80 km/h). Besides, with vehicle X it is deduced that the infiltration path does not go through the HVAC system. In other words, the vehicle speed does not influence the recirculation flap behaviour. The airflow due to high speed does not “push” the flap and does not create a leakage. Hence, it is likely that the

595 infiltrated air does not flow through the filter elements. Infiltration introduces polluted air into
596 the cabin.
597
598 The overall analysis of the results depicts a competition between the infiltration flow rate and
599 the fresh air flow rate driven by the blower. The fresh air driven by the blower behaves as a
600 shield against infiltration. However, in some cases the infiltration flow rate can overcome the
601 fresh air flow rate from the blower.
602
603
604 **5. Conclusions**
605 A tracer gas technique using CO_2 is used to evaluate the air exchange rate of a cabin vehicle.
606 The experiment performed on two vehicles shows that there is an additional flow rate inlet
607 into the cabin with higher vehicle speed. The ventilation setting also has a broad impact.
608 Beside the vehicle speed, the infiltration flow rate is triggered by recirculation mode and
609 upper blower position. In fresh air mode with an active blower, the cabin is in a positive
610 pressure mode that acts as a shield against infiltration. A number of enquiries are still active.
611
612 No other literature study is found to confirm the infiltration at the front of the cabin, or to
613 evaluate the infiltration of an electric vehicle. The architecture of an electric vehicle is much
614 different from a classic thermal engine vehicle (e.g. location of the engine, addition of a
615 battery pack). The infiltration process through the small gaps of the car body can be easily
616 impacted. Regarding gasoline engine vehicle (Y) no test is specifically performed in order to
617 locate the infiltration path. However driving this vehicle at high speed (with the ventilation
618 turned off) emphasises a clear feeling of airflow on the legs of the driver and the side
619 passenger. This infiltration airflow at the bottom front of the cabin is also perceived on other
620 personal vehicles in the same conditions. There is no evidence that it does not happen at the
621 rear back of the cabin as well.
622
623 Infiltration introduces non-filtered outside air directly into the cabin. Regarding the thermal
624 aspect (temperature, humidity) or air quality aspect (pollutants, particles) this is something
625 that should be avoided, or at least limited. It appears that at a given vehicle speed the best
626 strategy to avoid infiltration is to increase the amount of fresh air driven by the blower.
627 However, by doing so it also increases the amount of cold/hot air into the cabin, thus having a
628 negative impact on the energy aspect. Besides, it also increases the load on the filtration

system. A trade-off must be found in order to optimise both air quality and energy savings. In that purpose a new filtration system (Lesage et al., 2019a, 2019b) coupled with a smart control of the ventilation settings could be integrated in a vehicle.

Acknowledgements

The work in this article is done in a joint International Research Chair entitled "Filtration systems: fluid dynamics and energy consumption reduction" between MANN+HUMMEL and Ecole Centrale de Nantes. This research work is financially supported by the French Government and managed by the National Research Agency (ANR) with the Future Investments Program. The authors want to thank Antoine Bouedec and Julien Zenner for their contributions to the experiments.

References

Abi-Esber, L., El-Fadel, M., 2013. Indoor to outdoor air quality associations with self-pollution implications inside passenger car cabins. Atmospheric Environment 81, 450–463. https://doi.org/10.1016/j.atmosenv.2013.09.040

Baker, P.H., Sharples, S., Ward, I.C., 1987. Air flow through cracks. Building and Environment 22, 293–304. https://doi.org/10.1016/0360-1323(87)90022-9

Behrentz, E., Fitz, D.R., Pankratz, D.V., Sabin, L.D., Colome, S.D., Fruin, S.A., Winer, A.M., 2004. Measuring self-pollution in school buses using a tracer gas technique. Atmospheric Environment 38, 3735–3746. https://doi.org/10.1016/j.atmosenv.2004.04.007

Chan, A.T., Chung, M.W., 2003. Indoor–outdoor air quality relationships in vehicle: effect of driving environment and ventilation modes. Atmospheric Environment 37, 3795–3808. https://doi.org/10.1016/S1352-2310(03)00466-7

Chan, L.Y., Chan, C.Y., Qin, Y., 1999. The effect of commuting microenvironment on commuter exposures to vehicular emission in Hong Kong. Atmospheric Environment 33, 1777–1787. https://doi.org/10.1016/S1352-2310(98)00338-0

Clifford, M.J., Clarke, R., Riffat, S.B., 1997. Local aspects of vehicular pollution. Atmospheric Environment 31, 271–276. https://doi.org/10.1016/1352-2310(96)00205-1

Conceição, E., Silva, M.C.E., Viegas, D.X., 1997. Air quality inside the passenger compartment of a bus. Journal of exposure analysis and environmental epidemiology 7, 521–534.

Engelmann, R.J., Pendergrass, W.R., White, J.R., Hall, M.E., 1992. The effectiveness of stationary automobiles as shelters in accidental releases of toxic materials. Atmospheric Environment. Part A. General Topics 26, 3119–3125. https://doi.org/10.1016/0960-1686(92)90469-2

Fišer, J., Pokorný, J., 2014. Effect of car speed on amount of air supplied by ventilation system to the space of car cabin. EPJ Web of Conferences 67, 02027. https://doi.org/10.1051/epjconf/20146702027

672 Fletcher, B., Saunders, C.J., 1994. Air change rates in stationary and moving motor vehicles.
673 Journal of Hazardous Materials 14.
674 Fruin, S.A., Hudda, N., Sioutas, C., Delfino, R.J., 2011. Predictive Model for Vehicle Air
675 Exchange Rates Based on a Large, Representative Sample. Environ. Sci. Technol. 45,
676 3569–3575. https://doi.org/10.1021/es103897u
677 Harik, G., El-Fadel, M., Shihadeh, A., Alameddine, I., Hatzopoulou, M., 2017. Is in-cabin
678 exposure to carbon monoxide and fine particulate matter amplified by the vehicle's
679 self-pollution potential? Quantifying the rate of exhaust intrusion. Transportation
680 Research Part D: Transport and Environment 54, 225–238.
681 https://doi.org/10.1016/j.trd.2017.05.009
682 Heidt, F.D., Werner, H., 1986. Microcomputer-aided measurement of air change rates. Energy
683 and Buildings 9, 313–320. https://doi.org/10.1016/0378-7788(86)90036-8
684 Hudda, N., Fruin, S.A., 2013. Models for Predicting the Ratio of Particulate Pollutant
685 Concentrations Inside Vehicles to Roadways. Environ. Sci. Technol. 47, 11048–
686 11055. https://doi.org/10.1021/es401500c
687 Ireson, R.G., Easter, M.D., Lakin, M.L., Ondov, J.M., Clark, N.N., Wright, D.B., 2004.
688 Estimation of Diesel Particulate Matter Concentrations in a School Bus Using a Fuel-
689 Based Tracer: Sensitive and Specific Method for Quantifying Vehicle Contributions.
690 Transportation Research Record 1880, 21–28. https://doi.org/10.3141/1880-03
691 Knibbs, L.D., de Dear, R.J., Atkinson, S.E., 2009. Field study of air change and flow rate in
692 six automobiles. Indoor Air 19, 303–313. https://doi.org/10.1111/j.1600-
693 0668.2009.00593.x
694 Knibbs, L.D., Dear, R.J.D., Atkinson, S.E., 2007. Automobile hvac systems: Air flow,
695 leakage and their effects on in-vehicle air quality, in: IAQVEC 2007 Proceedings - 6th
696 International Conference on Indoor Air Quality, Ventilation and Energy Conservation
697 in Buildings: Sustainable Built Environment. Presented at the 6th International
698 Conference on Indoor Air Quality, Ventilation and Energy Conservation in Buildings:
699 Sustainable Built Environment, IAQVEC 2007, pp. 191–199.
700 Laussmann, D., Helm, D., 2011. Air Change Measurements Using Tracer Gases: Methods
701 and Results. Significance of air change for indoor air quality, in: Chemistry, Emission
702 Control, Radioactive Pollution and Indoor Air Quality, IntechOpen. Nicolas Mazzeo,
703 pp. 365–406.
704 Lee, E.S., 2013. Passenger Exposures to Ultrafine Particles and In-cabin Air Quality Control
705 (PhD thesis). UCLA, Los Angeles, USA.
706 Lee, E.S., Stenstrom, M.K., Zhu, Y., 2015a. Ultrafine particle infiltration into passenger
707 vehicles. Part II: Model analysis. Transportation Research Part D: Transport and
708 Environment 38, 144–155. https://doi.org/10.1016/j.trd.2014.11.005
709 Lee, E.S., Stenstrom, M.K., Zhu, Y., 2015b. Ultrafine particle infiltration into passenger
710 vehicles. Part I: Experimental evidence. Transportation Research Part D: Transport
711 and Environment 38, 156–165. https://doi.org/10.1016/j.trd.2015.04.025
712 Lesage, M., Del Fabbro, L., Le Nain, E., Migaud, J., Ebnet, D., Chalet, D., 2019a. Smart air
713 filtration for improved cabin air quality and energy savings in electric vehicles, in:
714 Outdoor and Indoor Air Pollution. Presented at the Atmos'Fair, Lyon, France.
715 Lesage, M., Del Fabbro, L., Migaud, J., Chalet, D., Le Nain, Eduin, E., Ebnet, D., 2019b.
716 Cabin air quality and energy savings in electric vehicles by using a smart filtration
717 system, in: FILTECH. Presented at the International Conference and Exhibition for
718 Filtration and Separation Technologies, Cologne, Germany.
719 Lv, Y., Wang, H., Wei, S., Wu, T., Liu, T., Chen, B., 2018. The experimental study on indoor
720 and outdoor penetration coefficient of atmospheric fine particles. Building and
721 Environment 132, 70–82. https://doi.org/10.1016/j.buildenv.2018.01.021

manufacturing, 2013. Follow the manufacturing of the ZOE.
Marshall, J.D., Behrentz, E., 2005. Vehicle Self-Pollution Intake Fraction: Children's Exposure to School Bus Emissions. Environ. Sci. Technol. 39, 2559–2563. https://doi.org/10.1021/es040377v
Mathai, V., Das, A., Bailey, J.A., Breuer, K., 2020. Airflows inside passenger cars and implications for airborne disease transmission. Sci.Adv. https://doi.org/10.1126/sciadv.abe0166
Migaud, J., Lesage, M., Chalet, D., Heininger, T., Bauer, B., Klein, M., 2018. Adaptive cabin air filter system for energy efficient filtration for e-vehicles, in: 18. Internationales Stuttgarter Symposium, Proceedings. Presented at the 18. Internationales Stuttgarter Symposium, Springer Fachmedien, Stuttgart, Germany, pp. 1115–1130. https://doi.org/10.1007/978-3-658-21194-3_86
Motor.TV, 2017. Car factory : Volkswagen e-golf production assembly line Wolfsburg.
Ott, W., Klepeis, N., Switzer, P., 2008. Air change rates of motor vehicles and in-vehicle pollutant concentrations from secondhand smoke. J Expo Sci Environ Epidemiol 18, 312–325. https://doi.org/10.1038/sj.jes.7500601
Ott, W., Switzer, P., Willits, N., 1994. Carbon Monoxide Exposures Inside an Automobile Traveling on an Urban Arterial Highway. Air & Waste 44, 1012–1018. https://doi.org/10.1080/10473289.1994.10467295
Park, J.H., Spengler, J.D., Yoon, D.W., Dumyahn, T.S., Lee, K.-L., Ozkaynak, H., 1998. Measurement of air exchange rate of stationary vehicles and estimation of in-vehicle exposure. J Expo Anal Environ Epidemiol 8, 65–78.
Petersen, G.A., Sabersky, R.H., 1975. Measurements of Pollutants inside an Automobile. Journal of the Air Pollution Control Association 25, 1028–1032. https://doi.org/10.1080/00022470.1975.10470174
PlaneteGT TV, 2019. Peugeot 208 2019 : Production backstage.
Quiros, D.C., Lee, E.S., Wang, R., Zhu, Y., 2013. Ultrafine particle exposures while walking, cycling, and driving along an urban residential roadway. Atmospheric Environment 73, 185–194. https://doi.org/10.1016/j.atmosenv.2013.03.027
Sherman, M.H., 1990. Tracer-gas techniques for measuring ventilation in a single zone. Building and Environment 25, 365–374. https://doi.org/10.1016/0360-1323(90)90010-O
Xu, B., Liu, S., Zhu, Y., 2010. Ultrafine particle penetration through idealized vehicle cracks. Journal of Aerosol Science 41, 859–868. https://doi.org/10.1016/j.jaerosci.2010.05.005
Zagury, E., 2000. Exposure of Paris taxi drivers to automobile air pollutants within their vehicles. Occupational and Environmental Medicine 57, 406–410. https://doi.org/10.1136/oem.57.6.406
Zhu, Y., Lee, E., 2015. Reducing air pollution exposure in passenger vehicles and school buses (No. 11–310). UCLA Fielding School of Public HEalth, California, USA.